Copyright © 1996 Elsevier Science Ltd
Paper No. 1962. (quote when citing this article)
Eleventh World Conference on Earthquake Engineering
ISBN: 0 08 042822 3

SEISMIC HAZARD AND GROUND MOTIONS ESTIMATES FOR A BUILDING SITE IN KOBE, JAPAN

F.I. MAKDISI, M.S. POWER, J.R. WESLING, K.L. HANSON, Z.-L. WANG, D. ROSIDI, S.J. CHIOU

Geomatrix Consultants, Inc. 100 Pine Street, 10th Floor,
San Francisco, California, U.S.A.

ABSTRACT

A magnitude Mw 6.9 earthquake struck the city of Kobe, Japan, on January 17, 1995. The earthquake resulted in over 5,000 fatalities and significant structural damage and destruction with estimated total losses on the order of 200 billion dollars. The earthquake occurred on the Nojima fault with an observed surface fault rupture of approximately 9 km on Awaji Island. The length of the rupture surface estimated from the aftershock zone was approximately 45 km.

This paper describes a study undertaken to evaluate the earthquake ground motions for purposes of a seismic evaluation of a building located on Rokko Island, about 5 km from the Nojima fault rupture. The subsurface soil conditions at Rokko Island consist of reclaimed soils overlying alluvial and marine deposits extending to depths of about 700 meters below existing ground surface. The ground motion studies included a seismotectonic evaluation and an assessment of the local and regional seismic sources significant to the site; an evaluation of the historical seismicity within the region; an evaluation of the maximum earthquakes associated with the significant seismic sources, as well as an assessment of their earthquake recurrence; and probabilistic and deterministic analyses to estimate expected earthquake ground motions at bedrock underlying the site. Ground response analyses were performed using one-dimensional wave propagation techniques to estimate the top-of-soil ground motions for the estimated outcropping rock motions. Ground motions also were computed at the site's ground surface using as input a recording (obtained during the Kobe earthquake) from a downhole array on neighboring Port Island, approximately 6 km west of the building site. The recording was obtained at a depth of 84 m below ground surface. The computed ground motions at the soil surface at the site were compared with ground motions recorded (during the same earthquake) at the basement of a nearby building. The computed and recorded results were found to be in fairly reasonable agreement.

Probabilistic estimates were made in terms of equal hazard response spectra associated with 10-percent probability of exceedance in 50 years (475-year return period) and in 100 years (950-year return period). Deterministic estimates were made for a number of significant seismic sources in the vicinity of the site. Controlling ground motions at the site (in the frequency range of interest to the building being evaluated) were from a maximum magnitude M_w 7.1 earthquake on the Kariya-Koyo fault at a distance of about 3.5 km from the building site. Comparisons are presented between the results of the deterministic and probabilistic estimates of ground motions.

KEY WORDS

Seismic hazard; earthquake ground motion; site response, design response spectra.

INTRODUCTION

This paper presents the results of a seismic hazard and ground motions study performed for a building site in Kobe, Japan. The results of this evaluation were used in a seismic assessment of the building located on Rokko Island, about 5 km from the Nojima Fault. The Nojima Fault was the source of the magnitude M_w 6.9 earthquake that struck the City of Kobe on January 17, 1995. The building is founded on a deep

piled foundation. The subsurface conditions at the site consist of reclaimed soils overlying alluvial and marine deposits to depths of about 700 meters below existing ground surface.

In the following sections of this paper we provide a characterization of the significant seismic sources in the site region; the results of the probabilistic seismic hazard analyses; deterministic estimates of the site bedrock motions due to the dominant nearby seismic sources, together with comparisons with the probabilistic equal hazard spectra; and the results of site response analyses performed to estimate top-of-soil ground motions for this deep soil site.

IDENTIFICATION AND CHARACTERIZATION OF SEISMIC SOURCES

The characterization of seismic sources was based on a review of published reports and maps (the Research Group for Active Faults of Japan, 1991, 1992), discussions with researchers knowledgeable in the region, and limited field reconnaissance that included a field trip along the Nojima fault, the Rokko fault system, and the Median Tectonic line. The seismic source parameters and associated weights (uncertainty) used in the hazard analyses for this study reflect judgment based on the above-mentioned data review and sources of information.

The principal seismic sources affecting the ground motions hazard at the site are listed in Table 1. The two principal seismic source types shown are the Nankai subduction zone sources and the nearby intraplate crustal sources. The Nankai subduction zone earthquakes consist of the Philippine Sea-Eurasian plate interface, and earthquakes occurring within the subducting Philippine Sea Plate, called intraslab earthquakes. Interface earthquakes of the Nankai subduction zone are located about 108 km from the building site, their estimated maximum magnitude ranged between 8.3 and 8.9, with a value of 8.75 used in the deterministic analysis. Intraslab events are located at a closest distance of about 77 km from the building site with estimated maximum magnitude in the range of 7 to 7½, with a maximum value of 7½ used for the deterministic analysis.

The nearby Eurasian crustal sources include the Rokko Fault System with faults at a closest distance to the site between 3 and 5 km; and the Median Tectonic Line located at about 45 km from the building site. The Rokko fault system appears to be part of a larger fault system that is about 80 to 100 km long and is comprised of at least three subparallel, northeast-striking, right-lateral strike-slip or oblique-slip faults, that include the Nojima-Gosukebashi Fault, the Kariya-Koyo Fault, and the Osaka Bay Fault. Maximum magnitudes for earthquakes on these faults were estimated to range between 6.8 and 7.1. The Nojima-Gosukebashi Fault system ruptured during the M_W 6.9 Hyogo-ken Nabu (Kobe) Earthquake of January 17, 1995. The Median Tectonic Line is a steeply dipping to vertical right-lateral strike slip fault. The fault is located at a closest distance of about 45 km from the building site with estimated maximum magnitude of about 7.3.

Estimates of the maximum magnitude for the subduction zone sources were based on estimated dimensions of the maximum rupture and published empirical correlations between rupture dimensions and earthquake magnitude. The relationships of Abe (1981, 1984) and Geomatrix (1995) were used for this assessment. The estimates of the maximum magnitude for intraslab sources was based on data from similar seismically active margins. For the Eurasian Crustal sources, maximum magnitudes were determined using the relationships of Wells and Coppersmith (1994). In these relationships the maximum magnitude is related to the subsurface rupture length or to the rupture area. For the probabilistic analysis, the final result of the estimation of maximum magnitude is a probabilistic distribution of magnitudes for each source that reflects the uncertainties in rupture parameters and judgments about these parameters. These rupture parameters are listed in Table 2 for four seismic sources considered most significant to the ground motion hazard at the site. The maximum magnitude estimates for the deterministic analysis as given in Table 1 represent best-judgment values based on available rupture estimates including all pertinent relationships.

ASSESSMENT OF EARTHQUAKE RECURRENCE

The probabilistic seismic hazard analysis procedure requires the specification of an earthquake recurrence relationship for each seismic source, defining the frequency of occurrence of various magnitude earthquakes up to the maximum magnitude possible on the sources. For specific crustal faults identified in this assessment, recurrence was estimated on the basis of geologic slip rates. For the primary crustal sources

affecting the seismic hazard at the Building site, the estimated slip rates are presented in Table 2. A characteristic earthquake recurrence model (Youngs and Coppersmith, 1985) was used to determine the relative magnitude distribution of the recurrence relationships for identified crustal faults. For regional areal crustal source zones (which contribute little to the hazard at the building site compared to the nearby crustal faults), recurrence was assessed based on analyses of seismicity data. For large interface subduction zone earthquakes, recurrence was assessed based on the historical record of large plate-boundary earthquakes; it was assumed that all significant moment release was associated with occurrence of characteristic large earthquakes. Recurrence rates for the intraslab subduction zone earthquakes were estimated based on the analyses of observed seismicity.

PROBABILISTIC SEISMIC HAZARD ANALYSIS RESULTS

The basic elements for a probabilistic seismic hazard analysis are: (a) identification of potential active seismic sources; (b) specification of earthquake recurrence relationships for each source; (c) specifications of attenuation relationships defining ground motion levels as a function of earthquake magnitude and distance from rupture source; and (d) calculation of the probability of exceedance of peak acceleration and response spectral accelerations using input from the elements above, and development of equal hazard response spectra. Attenuation relationships used in the analyses for rock motions for the crustal earthquake sources included: (1) relationships for spectral shapes based on Kawashima et al. (1984), scaled to the peak ground acceleration values determined from Fukushima (1994); (2) relationships of Sadigh et al. (1993); and (3) relationships of Idriss (1991), with updated standard deviation from Idriss (1994). For subduction zone sources the relationships of Geomatrix (1995) were used in the analysis.

The seismic hazard was computed for 29 crustal fault sources, the two distant subduction zone sources, and 9 areal source zones. The crustal sources are shown on Figure 1. The results of the seismic hazard analysis are presented on Figure 2 in terms of the annual frequency of exceedance for peak rock acceleration and 5 percent damped response spectral values for structural periods of 0.2 and 2.0 seconds. The mean hazard curves and uncertainty bands (5^{th} to 95^{th} percentiles) also are shown. Figure 3 shows the contributions of the significant seismic sources to the total hazard curves. The fault identification numbers and corresponding fault locations can be found on Figure 1. At the higher acceleration levels, the local crustal faults dominate the ground motion hazard at the building site.

DETERMINISTIC ESTIMATES OF ROCK GROUND MOTIONS

Deterministic estimates of rock outcrop ground motions at the site were made for the nearby crustal sources listed in Table 1. Figure 4 shows predicted median (5 percent damped) rock spectra at the site for maximum earthquakes on these primary crustal sources. Figure 4 shows that ground motions at the site (particularly in the long-period range) are controlled by the M_W 7.1 earthquake on the Kariya-Koyo fault located at a distance of 3.5 km away. Accordingly, results of the deterministic estimates are presented for ground motions associated with the maximum earthquake on this fault. The results of the deterministic and probabilistic estimates of rock motions at the site are compared in Figure 5. In this figure median and 84^{th} percentile deterministic rock spectra are compared with probabilistic equal hazard spectra associated with 10-percent probability of exceedance in 50 years (475-year return period) and in 100 years (950-year return period). The results in Figure 5 show that the deterministic median rock spectrum corresponds approximately to the 950-year return period hazard spectrum, at structural periods between about 0.5 and 3 seconds.

TOP-OF-SOIL GROUND MOTIONS

As mentioned earlier the building site on Rokko Island is located on deep soil conditions extending to depths of about 700 m below existing ground surface. The soil profile within the top 100 meters consists of about 25 meters of medium dense sandy fill with a shear wave velocity of about 320 m/sec. Underlying the sandy fill is an alluvial clay layer about 15 m thick with a shear wave velocity of about 190 m/sec. Underlying the clay layer and extending to a depth of about 100 meters are interbedded alluvial dense sands and stiff clays with measured shear wave velocities varying between 300 and 400 m/sec. Underlying this depth are the upper and lower Osaka Group formations that extend to about 700 m below ground surface where the shear wave velocity is about 700 m/sec. To estimate ground motions at the soil surface for this site, one-dimensional site response analyses were performed and transfer functions were developed between the

bedrock motions and top-of-soil motions. Estimates of top-of-soil spectra (using appropriately developed transfer functions) for the nearby maximum earthquake are shown on Figure 6 and are compared with the input rock spectra. The comparison in this figure shows the longer period amplification of the rock motions and the short period deamplification for this deep soil profile. The short period deamplification may be overstated because of the use of the SHAKE program.

Recordings were obtained during the 1995 Kobe earthquake at a downhole array on nearby Port Island, approximately 6 km west of the building site. These records were obtained at the ground surface and at depths of about 17 m, 33 m, and 84 m below ground surface. The record obtained at 84 m was used as input in a site response analysis at the Building site (on Rokko Island) to obtain ground motions at the soil surface. The input motion (from Port Island at 84 m) was scaled for the effects of distance and applied as an interface motion in the site response analysis. Ground motions, computed at the surface for the average of the two horizontal components, are compared with the estimated deterministic (median and 84th percentile) top-of-soil motions on Figure 7. These estimates are also compared with response spectra computed from a recording obtained in the basement of a nearby building on Rokko Island during the 1995 Kobe earthquake. The average spectra of the recorded ground motions in the long period range are in fairly close agreement with the median site-specific spectrum estimated from ground response analyses.

ACKNOWLEDGEMENT

A number of researchers provided input that contributed to our understanding of the seismic sources in the Kobe area: Dr. K. Huzita, Fault Research Data Center, Osaka; Dr. R. Hyndman, Geological Survey of Canada; Dr. T. Nakata, Hiroshima University; Dr. A. Okada, Kyoto University; Dr. S. Masato, Suncoh Consultants; and Dr. R. Yeats, Oregon State University. Dr. Y. Iwasaki, Geo-Research Institute, and Drs. Kenji and Ann Mori, Kiso-Jiban Consultants, graciously provided copies of ground motion records from the Kobe earthquake. The contributions of these individuals are gratefully acknowledged.

REFERENCES

Abe, K. (1981). Magnitude of large shallow earthquakes from 1904-1980, *Physics of the Earth and Planetary Interiors*, vol. 27, p. 72-92.

Abe, K. (1984). Complements to "Magnitudes of large shallow earthquakes from 1904-1980," *Physics of the Earth and Planetary Interiors*, vol. 34, p. 17-23.

Fukushima,(1994). Theory of the generation and propagation of seismic waves, empirical prediction of strong ground motions, ORI Research paper, Ohsaki Research Institute, Shimizu Corporation, in Japanese.

Geomatrix Consultants (1995). Seismic design mapping, State of Oregon, Final Report.

Idriss, I.M., (19991). Procedures for selection earthquake ground motions at rock sites, A Report to U.S. Department of Commerce, NIST GCR 93-625, September.

Idriss, I.M., (1994). Personal communication, Revised Standard Error Terms.

Kawashima, K. et al. (1984). Attenuation of peak ground motion and absolute acceleration response spectra, 8th World Conference on Earthquake Engineering, San Francisco, Vol. 11.

Sadigh, K. et al. (1993). Specification of long-period ground motion: Updated attenuation relationships for rock site conditions and adjustments factors for near-fault efffects, ATC-17-1 Seminar on Seismic Isolation, Passive Energy Dissipation, and Active Control, San Francisco, March 11-12.

The Research Group for Active Faults in Japan (1991). Active faults in Japan: Sheet maps and inventories (revised edition), *University of Tokyo Press*, Tokyo, 437 p.

The Research Group for Active Faults in Japan (1992). Maps of active faults in Japan with explanatory text, *University of Tokyo Press*, Tokyo, 73 p.

Wells, D.L., and Coppersmith, K.J., (1994). New empirical relationships among magnitude, rupture length, rupture area, and surface displacement: Bulletin of the Seismological Society of America, v. 84, p. 974-1002.

Youngs, R.R., and K.J. Coppersmith (1985b). Implications of fault slip rates and earthquake recurrence models to probabilistic seismic hazard estimates, *Bulletin of the Seismological Society of America*, vol. 75, p. 939-964.

Table 1. Primary Earthquake Sources

Earthquake Source	Closest Source-to-Site Distance (km)	Magnitude Earthquake Magnitude
Osaka Bay Fault	2.8	6.8
Nojima-Gosukebashi Fault System	5.0	6.9
Kariya-Koyo Fault System	3.5	7.1
Median Tectonic Line	45	7.3
Interface Event-Nankai Subduction Zone	108	8.75
Intraslab Event-Nankai Subduction Zone	77	7.5

Table 2. Seismic Source Characteristics--Crustal Sources

Fault[1]		Fault No.[2]	Style[3]	Total Length (km)	Downdip Geometry	Seismogenic Depth (km)[4]	Rupture Length (km)[4]	Slip Rate (mm/yr)[4]
Nojima-Gosukebashi Fault System (81-15; 76-66, -79 & -80)		1	SS	67	90°	12 (0.3) 15 (0.5) 18 (0.2)	30 (0.2) 45 (0.6) 60 (0.2)	1.0 (0.4) 1.2 (0.4) 1.5 (0.2)
Kariya-Koyo Fault System (81-3; 76-64, -79, & -80)		2	SS	100	90°	12 (0.3) 15 (0.5) 18 (0.2)	45 (0.3) 60 (0.4) 80 (0.2) 100 (0.1)	1.0 (0.3) 1.5 (0.5) 2.0 (0.2)
Osaka Bay- (Models 3a & 3b based on closest distance) (77-S1)	5.5 km (0.5)	3a	SS	55	90°	12 (0.3) 15 (0.5) 18 (0.2)	30 (0.4) 40 (0.4) 50 (0.2)	0.7 (0.3) 1.0 (0.6) 1.5 (0.1)
	2.8 km (0.5)	3b						
Median Tectonic Line (81-12)		4	SS	250	90°	12 (0.3) 15 (0.5) 18 (0.2)	45 (0.1) 65 (0.4) 80 (0.3) 105 (0.1) 250 (0.1)	1.0 (0.5) 3.0 (0.5)

Notes:

[1] Number in parentheses refers to fault number in The Research Group on Active Faults of Japan (1991).
[2] See Figure 1 for location of fault source.
[3] Style of faulting: SS = Strike-Slip Fault; R = Reverse Fault.
[4] Values in parentheses are subjective relative likelihoods or weights.

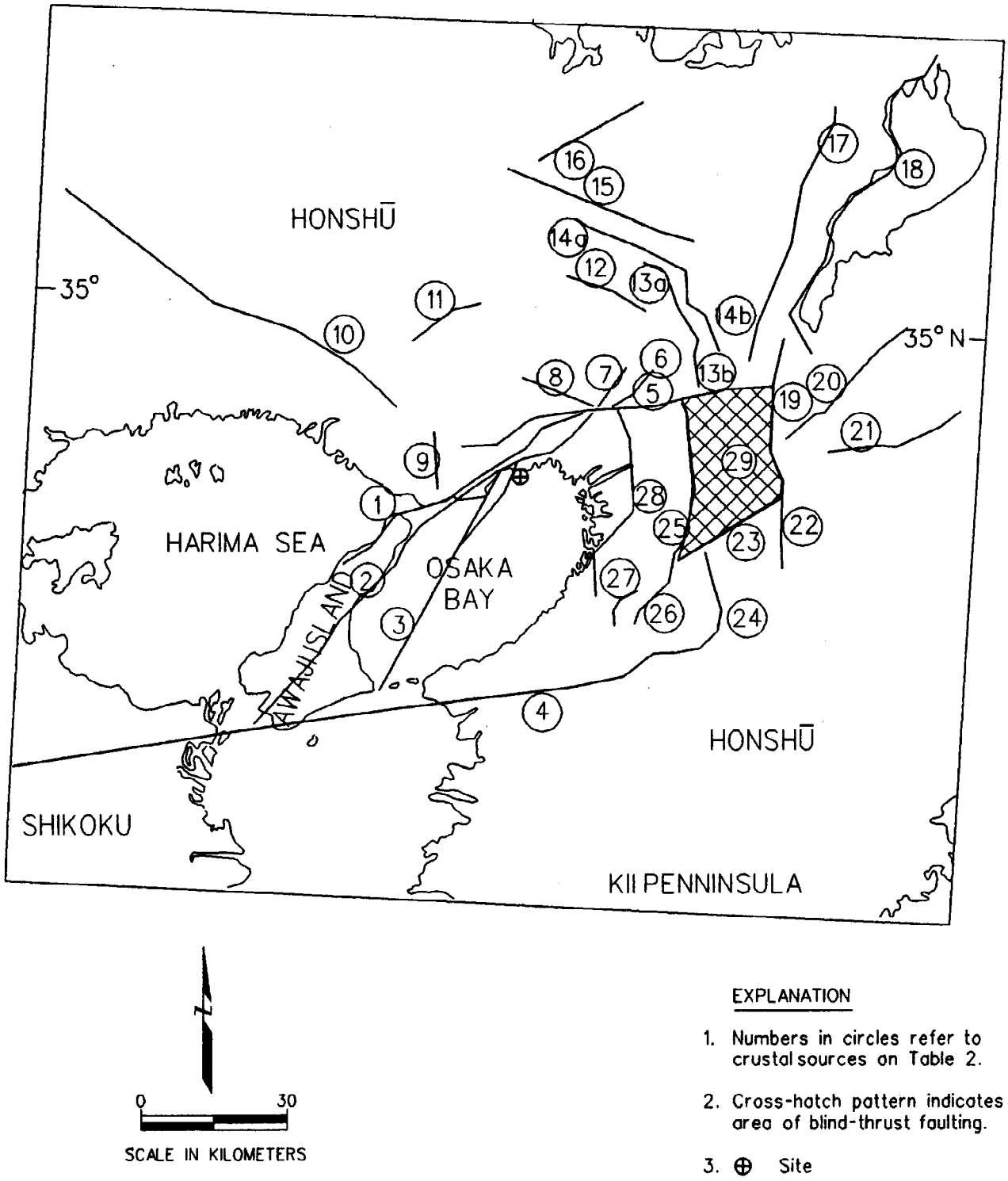

Fig. 1. Seismic source map.

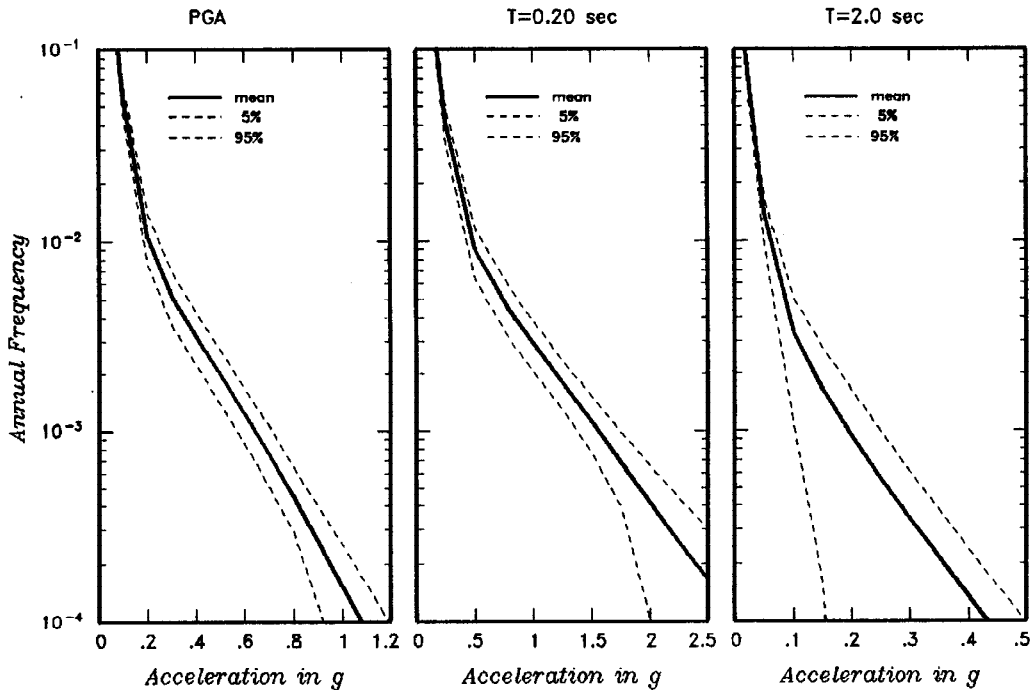

Fig. 2. Probabilistic hazard curves at rock outcrop for peak acceleration and response spectral ordinates (5% damping).

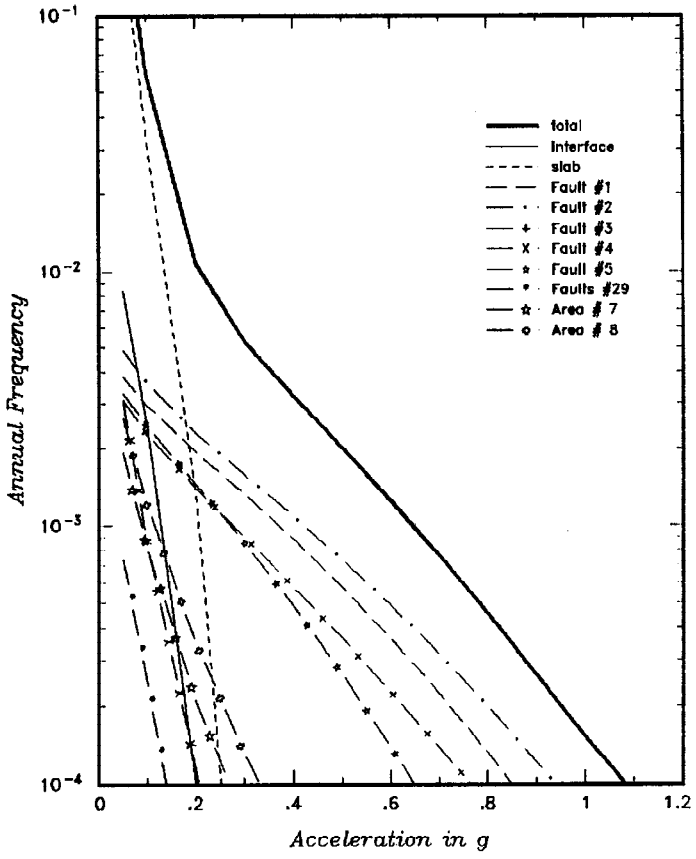

Fig. 3. Contributions of various seismic sources to the total hazard curve (peak rock acceleration).

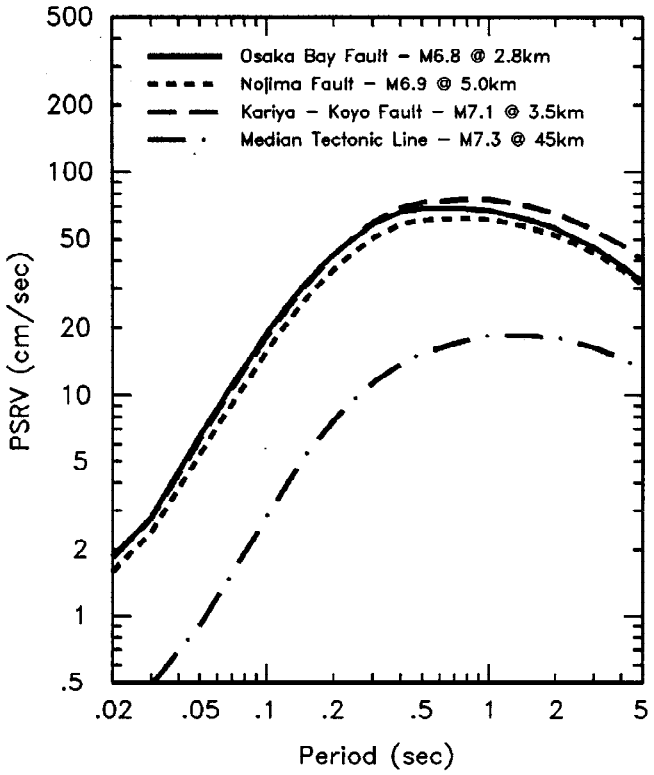

Fig. 4. Predicted median rock spectra for primary crustal fault sources

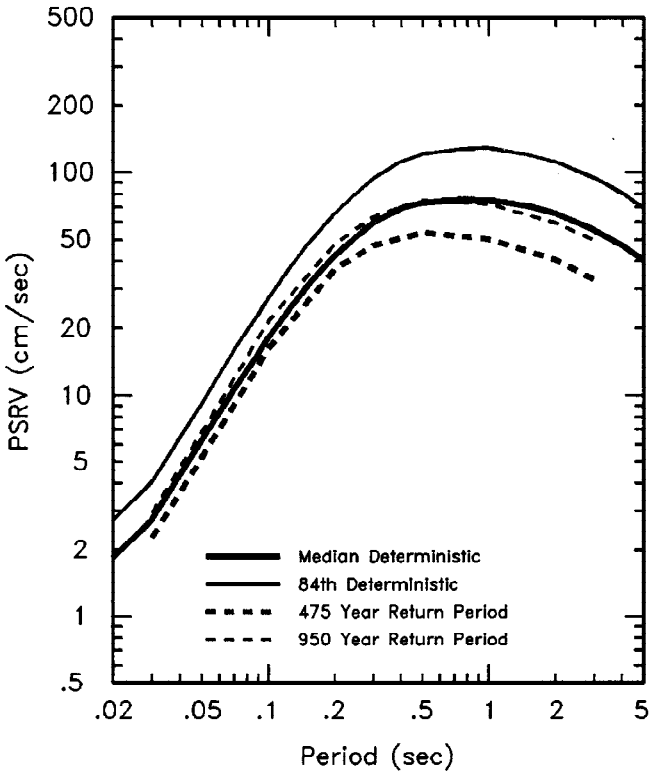

Fig. 5. Comparison between deterministic and probabilistic rock outcrop spectra

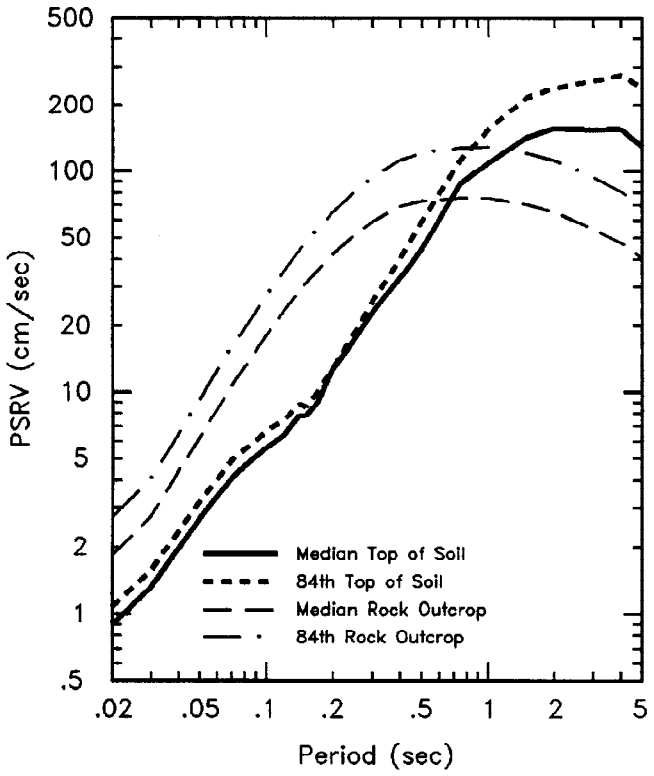

Fig. 6. Comparison of top-of-soil motions calculated at site with input rock spectra for nearby maximum earthquake

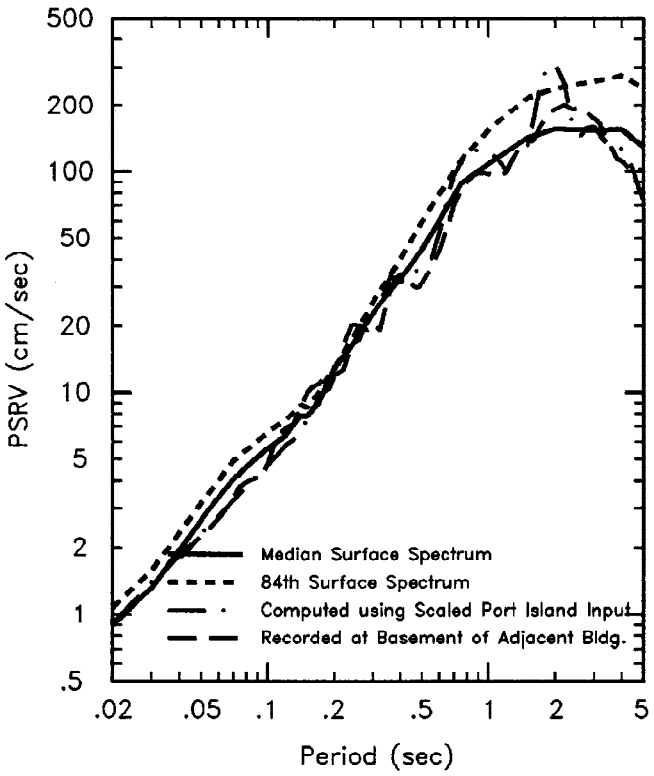

Fig. 7. Comparison of predicted deterministic top-of-soil motions with computed and recorded ground motions